



<http://www.diva-portal.org>

This is the published version of a paper published in .

Citation for the original published paper (version of record):

Liu, T., Li, G., Shen, N., Wang, L., Timmer, B J. et al. (2021)
Isolation and Identification of Pseudo Seven-Coordinate Ru(III) Intermediate
Completing the Catalytic Cycle of Ru-bda Type of Water Oxidation Catalysts
CCS Chemistry, : 2612-2621
<https://doi.org/10.31635/ccschem.021.202101159>

Access to the published version may require subscription.

N.B. When citing this work, cite the original published paper.

Permanent link to this version:

<http://urn.kb.se/resolve?urn=urn:nbn:se:kth:diva-302712>

Isolation and Identification of Pseudo Seven-Coordinate Ru(III) Intermediate Completing the Catalytic Cycle of Ru-bda Type of Water Oxidation Catalysts

Tianqi Liu^{1†}, Ge Li^{2†}, Nannan Shen^{3†}, Linqin Wang⁴, Brian J. J. Timmer¹, Shengyang Zhou⁵, Biaobiao Zhang⁴, Alexander Kravchenko¹, Bo Xu¹, Mårten S. G. Ahlquist² & Licheng Sun^{1,4,6*}

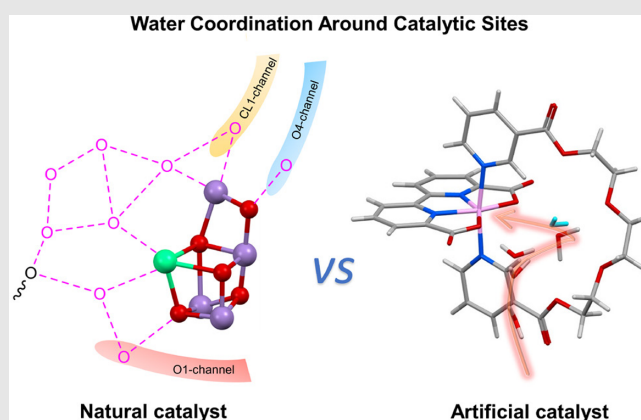
¹Department of Chemistry, School of Engineering Sciences in Chemistry, Biotechnology, and Health, KTH Royal Institute of Technology, Stockholm 10044, ²Department of Theoretical Chemistry and Biology, School of Engineering Sciences in Chemistry, Biotechnology, and Health, KTH Royal Institute of Technology, Stockholm 10691, ³State Key Laboratory of Radiation Medicine and Protection, School for Radiological and Interdisciplinary Sciences (RAD-X), Collaborative Innovation Center of Radiation Medicine of Jiangsu Higher Education Institutions, Soochow University, Suzhou 215123, ⁴Center of Artificial Photosynthesis for Solar Fuels, School of Science, Westlake University, Hangzhou 310024, ⁵Nanotechnology and Functional Materials, Department of Materials Sciences and Engineering, The Ångström Laboratory, Uppsala University, Uppsala 75103, ⁶Institute of Artificial Photosynthesis (IAP), State Key Laboratory of Fine Chemicals, Dalian University of Technology (DUT), Dalian 116024

*Corresponding author: lichengs@kth.se; [†]T. Liu, G. Li, and N. Shen contributed equally to this work.

Cite this: *CCS Chem.* **2021**, *3*, 2612–2621

Isolation of Ru^{III}-bda (17-electron specie) complex with an aqua ligand (2-electron donor) is challenging due to violation of the 18-electron rule. Although considerable efforts have been dedicated to mechanistic studies of water oxidation by the Ru-bda family, the structure and initial formation of the Ru^{III}-bda aqua complex are still controversial. Herein, we challenge this often overlooked step by designing a pocket-shape Ru-based complex 1. The computational studies showed that 1 possesses the crucial hydrophobicity at the Ru^V(O) state as well as similar probability of access of terminal O to solvent water molecules when compared with classic Ru-bda catalysts. Through characterization of single-crystal structures at the Ru^{II} and Ru^{III} states, a pseudo seven-coordinate “ready-to-go” aqua ligand with Ru^{III}...O distance of 3.62 Å was observed. This aqua ligand was also found to be part of a formed hydrogen-bonding network, providing a

good indication of how the Ru^{III}-OH₂ complex is formed.



Keywords: Ru-bda, water oxidation, pseudo seven-coordinate, Ru^{III}-OH₂ intermediate, water preorganization

Introduction

Splitting water into hydrogen and oxygen is a promising strategy to store solar energy in the form of chemical bonds.^{1,2} However tempting this strategy is, its implementation is still limited by the sluggish kinetics of the four-electron catalytic water oxidation process.³ Significant advances in catalytic water oxidation have been achieved since the first well-characterized Ru-based water oxidation catalyst blue dimer was reported.⁴ Blue dimer features two Ru^{III}-aqua centers being bridged by an oxo group, as shown in Chart 1, where the aqua ligand provides protons for the subsequent proton-coupled electron transfer (PCET) steps to achieve redox-potential leveling. A subsequent report has shown that a single catalytic site complex with a bonded aqua ligand, Ru-tnp-OH₂, is also capable of catalyzing water oxidation, although the turnover frequency (TOF) was on the order of 10⁻² s⁻¹.⁵ The emergence of nonaqua ruthenium complex Ru-bda is a milestone for the field, and its catalytic efficiency is comparable with that of photosystem II.⁶⁻¹⁶ The superiority of Ru-bda mainly originates from negatively charged backbone ligands and its variable coordination number at different oxidation states.¹⁷⁻¹⁹ In detail, six-coordinate Ru-bda was proposed to form its aqua adduct in the presence of water, thanks to which Ru-aqua complex can be oxidized to the reactive seven-coordinate Ru^V(O)

species at a low overpotential (200 mV). Subsequently, a great number of Ru-bda analogues such as Ru-tda, Ru-bpaH₂, and Ru-bds have been designed for efficient Ce^{IV}-driven/electrocatalytic water oxidation.²⁰⁻²⁴ It is noteworthy that Ru-tda and Ru-bds demonstrated impressively high activity for electrocatalytic water oxidation (TOF is on the order of 10⁵ s⁻¹), while the incomplete formation of the catalytically active Ru-aqua species of Ru-tda due to competitive carboxylate coordination was considered a significant drawback of this catalyst.²⁵ In addition to Ru-bda, other polypyridyl-based nonaqua ruthenium complexes have also been reported to behave as water oxidation catalysts.²⁶⁻³⁰ Overall, binding of the aqua ligand and its oxidation to metal-oxo/oxyl are elementary steps of water oxidation required for any kind of catalysts, and are often overlooked.³¹ Even for the state-of-the-art Ru-bda family, there is still a long-standing question, that is, the structure of Ru-aqua complex at low oxidation state. In consequence, a thorough understanding of the following PCET steps has been impeded. To allow rational improvement of water oxidation catalysts, it is indispensable to detail how the aqua ligand is presented to the active center.

Based on in-depth experimental and computational studies, nonaqua ruthenium complexes such as Ru-bda have served as invaluable platforms for advancing our understanding of water coordination at the initial step.

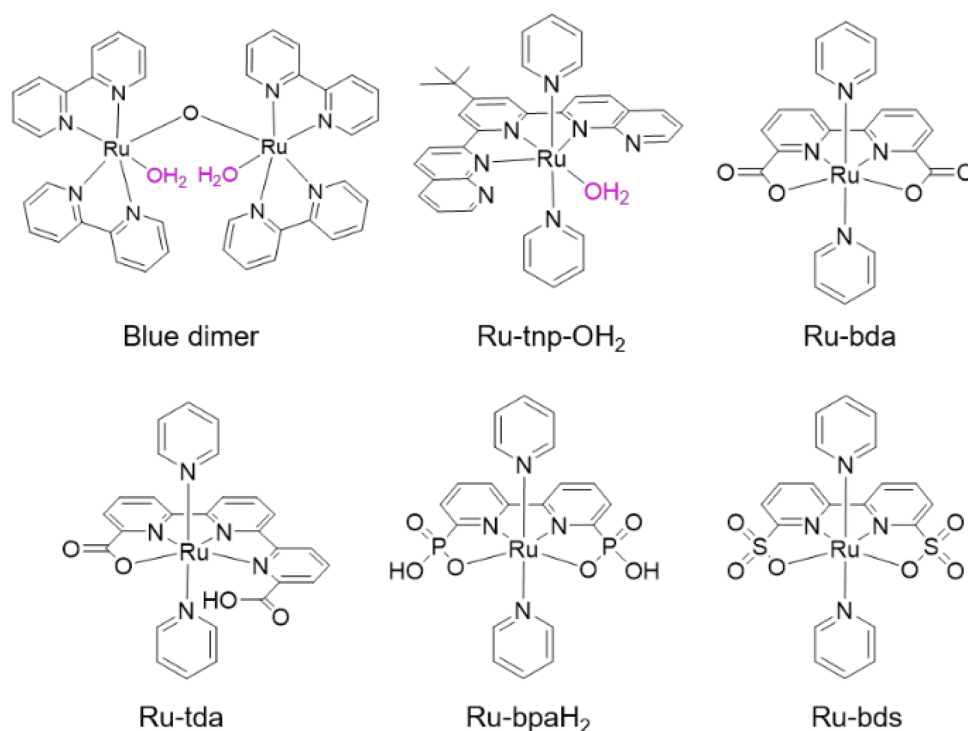


Chart 1 | Chemical structures of landmark Ru-based water oxidation catalysts. tnp: 4-tert-butyl-2,6-di(1,8-naphthylidin-2-yl)pyridine; bda2-: 2,2'-bipyridine-6,6'-dicarboxylate; tda2-: 2,2':6,2'-terpyridine-6,6'-dicarboxylate; bpaH₂2-: 2,2'-bipyridine-6,6'-diylbis(hydrogen phosphonate); bds2-: 2,2'-bipyridine-6,6'-disulfonate.

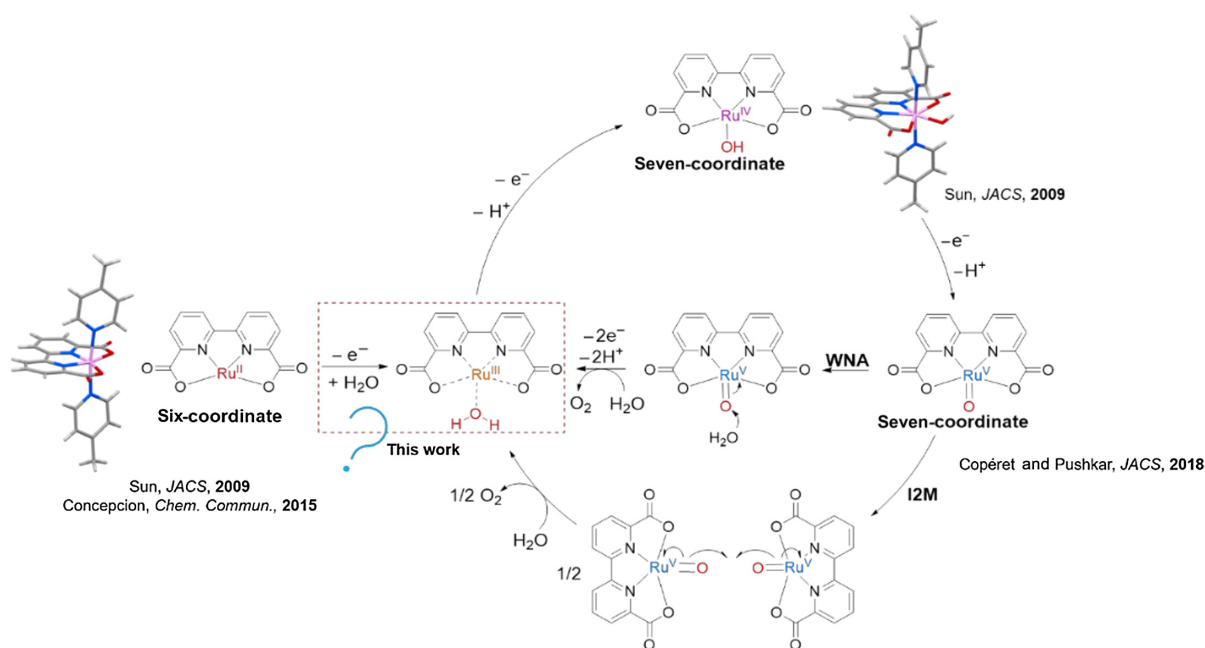


Figure 1 | Catalytic cycle of Ru-bda-based water oxidation catalysts. Axial ligands are omitted for clarity.

In this series, the coupling between two $\text{Ru}^{\text{V}}(\text{O})$ species or oxidizing $\text{Ru}^{\text{IV}}(\text{OH})$ to $\text{Ru}^{\text{V}}(\text{O})$ have been proposed as the rate-determining step (RDS), as shown in Figure 1.^{6,32} The highest TOF values observed so far are on the order of 10^3 s^{-1} , which means the catalysis operates on the microsecond time scale.³³ Accordingly the other steps in the catalytic cycle such as water coordination should theoretically be faster than the RDS. Thus, it is challenging to observe a water coordination step that occurs on a short time scale experimentally. The structures of six-coordinate $\text{Ru}^{\text{II}}\text{-bda}$ and seven-coordinate $\text{Ru}^{\text{IV}}(\text{OH})\text{-bda}$ have been clearly characterized by X-ray diffraction studies,³⁴ and the seven-coordinate $\text{Ru}^{\text{V}}(\text{O})\text{-bda}$ has also been detected recently by in situ X-ray absorption spectroscopy (XAS), as shown in Figure 1.³⁵ As the only missing part in the catalytic cycle, the coordination sphere of $\text{Ru}^{\text{III}}(\text{OH}_2)$ that provides access to the catalytic cycle, has been previously assigned to six-coordinate, or equilibrium between six- and seven-coordinate species according to the electron paramagnetic resonance (EPR) and XAS studies.^{36–38} However, solid evidence of $\text{Ru}^{\text{III}}\text{-bda}$ bearing an aqua ligand (e.g., X-ray crystal structures) has never been provided.

A well-established method to observe aqua ligand transfer pathways is to capture the surrounding water molecules³⁹ by engineering the secondary coordination sphere because the interactions with the local aqueous environment are controlled by a subtle interplay of weak intermolecular contacts. Unfortunately, discovery of preorganized water molecules in the second coordination sphere still relies heavily on serendipity. For example, a network of water molecules was found at the crystal lattice of a Ru water oxidation complex; however,

the role of these water molecules was ambiguous due to the long distance between Ru and O.²⁰ Introduction of a pocket-type secondary coordination sphere is a promising strategy to preorganize substrates within confined spaces through noncovalent interactions (NCIs).^{32,40,41} Würthner et al.³² reported a macrocyclic Ru complex which, according to computational studies, facilitated preorganization of up to 10 water molecules inside the formed pocket at the Ru^{IV} state. The follow-up studies provided the crystal structure of this macrocycle at the Ru^{II} state, but the initial catalytic state of $\text{Ru}^{\text{III}}\text{-aqua}$ complexes has not yet been revealed.^{41,42} Overall, insufficient understanding of the secondary coordination sphere and the lack of suitable secondary ligands have imposed a great challenge on the observation of Ru-aqua structures in low oxidation states.

Herein, a bio-inspired Ru-based catalyst **1** with a hydrophilic pocket is synthesized (Chart 2), where the pocket ligand provides a microenvironment to mimic the secondary coordination sphere of the oxygen-evolving complex (OEC) in photosystem II. This catalyst design was hypothesized to afford the necessary stabilization of the preorganized seven-coordinate aqua ligand to allow for its characterization. Spectroscopic, structural, and electrochemical studies in concert with computational results reveal that this pocket-type water oxidation catalyst could hold a “ready-to-go” aqua at the Ru^{III} oxidation state as a pseudo seven-coordinate ligand with minimal structural rearrangement, shedding light on details of the key water coordination step.

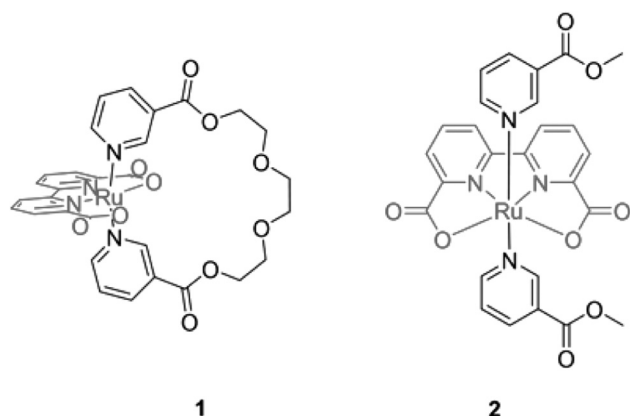


Chart 2 | Chemical structures of **1** and **2**.

Experimental Methods

Synthesis and characterization

Complex **1** and **2** were prepared following slightly modified literature procedures.^{34,43} In short, the desired catalyst was prepared by refluxing a degassed mixture of Ru(bda)(DMSO)₂ (DMSO = dimethyl sulfoxide) and the axial ligand in methanol over 4 h under N₂. The catalyst was obtained through flash column chromatography as reddish-brown powder and characterized by NMR and high-resolution mass spectroscopy (HRMS; Figure 2 and Supporting Information Figure S1–S4; for details, see Supporting Information). The X-ray crystallographic data (Supporting Information Table S1)

for the structures reported in this article have been deposited at the Cambridge Crystallographic Data Centre (CCDC) with the numbers of CCDC 1955358 and 1986038. These data can be obtained free of charge from the CCDC via www.ccdc.cam.ac.uk/data_request/cif

Results and Discussion

Characterization of Ru^{II} complex

The retention of the symmetry of molecule **1** is evident from the ¹H NMR spectra, exhibiting only three signals for the bda backbone unit (H_a, H_b, and H_c) and four signals for the axial ligand (H_d, H_e, H_f, and H_g). As previously observed, this symmetry can be easily disturbed by adding acetonitrile to the solution of **1** (Supporting Information Figure S5), splitting the protons from the bda unit into two separate peaks. This indicates that the cyclic ligand does not prevent incoming small molecules from coordinating with the Ru center. In contrast, the obtained crystal structure of **1**·H₂O shows an imperfect symmetrical structure with the axial macrocyclic ligand rotated away from the vertical axis by around 22.8° (Figure 3b), suggesting dynamic behavior of the axial ligand of **1** in solution.

Significant insights into the catalyst conformation can be gained by comparing the ¹H NMR spectra of **1** and reference molecule **2** (Figure 2). Similar chemical shifts in the aromatic region were observed except for H_d and H_g, which are located at the ortho position of the axial pyridine ligands. It is possible that the axial ligands linked together by a triethylene glycol unit form a rigid

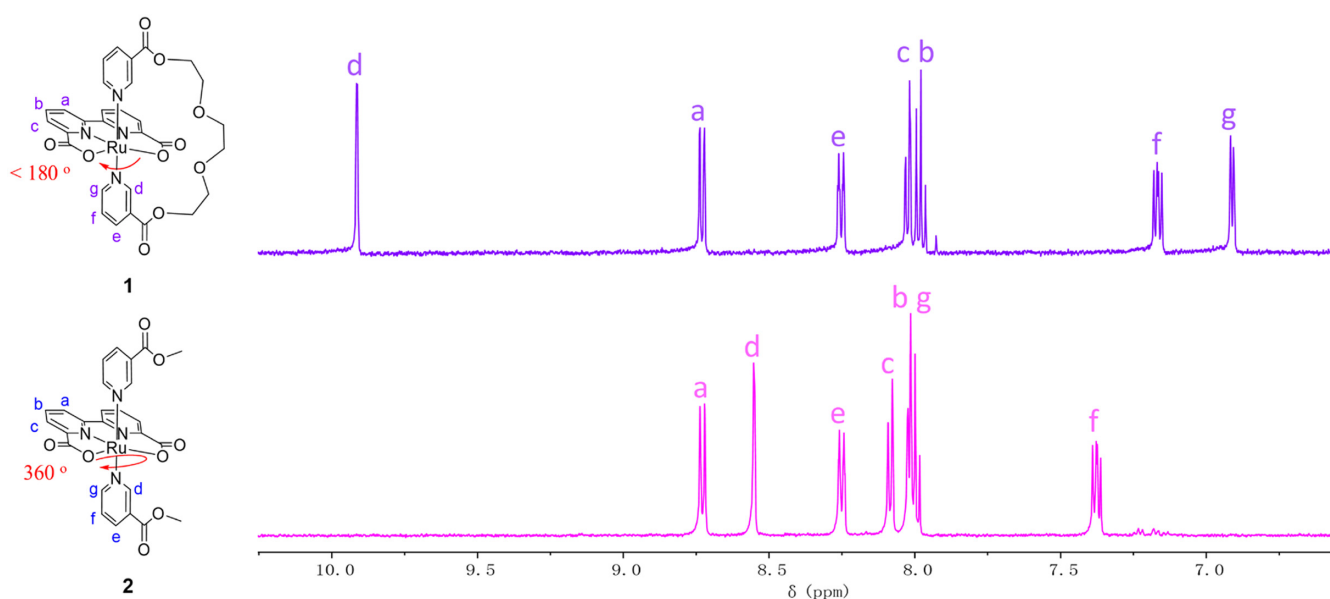


Figure 2 | ¹H NMR spectra of **1** (upper) and reference molecule **2** (lower) in CD₃OD.

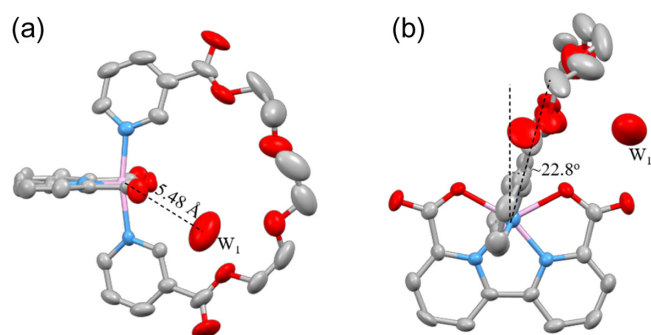


Figure 3 | Single-crystal structure of complex **1·H₂O** [(a) side view and (b) top view] with thermal ellipsoids at 50% probability. Hydrogen atoms are omitted for clarity. Color code: Ru, pink; O, red; N, blue; C, grey.

hydrophilic cavity, allowing the axial ligand to rotate only within a certain angle around the vertical axis at the front face of **1**. As a result, H_g is permanently located in the ring current of the bda-ligand and is thus more shielded, whereas H_d is located in the electronegative pocket deshielding these protons in comparison to the freely rotating ligand from **2**. The meta and para positions (H_f and H_e) are more distant and are thus less affected by the ring current of the bda unit. We hypothesize that in solution the dynamic behavior of the macrocyclic axial ligand of **1** is limited to left-to-right switching in front of the catalyst active site, whereas the axial ligand of **2** can rotate freely.

The single-crystal structures for **1·H₂O** are displayed in Figure 3, showing the macrocyclic ligand locates in front of the bda unit. Density functional theory (DFT) calculations (Supporting Information Figure S6) show that there is an energy difference of 9.62 kcal/mol between the front and back conformation, suggesting a 10⁷ times higher probability of the ethylene-glycol linker residing in front of the active site. The crystal structure of **1·H₂O** displays a typical distorted octahedral geometry around the Ru center with the O–Ru–O angle of 122.9°, which is similar to the previously reported conformation of Ru(bda)pic₂.³⁴ This large accessible site plays a critical role by allowing coordination of substrate water to form seven-coordinate Ru intermediates. Due to the relatively small linker size, the axial pyridyl ligands are slightly bent away, giving a minor difference for the N_{axial}–Ru–N_{axial} angle of 169.0° for **1·H₂O** compared to 173.0° for Ru(bda)pic₂. A single water molecule is found to be present in the crystal lattice, which is located between the bda-carboxyl and ether linkages of macrocyclic ligand. Notably, besides residual water from methanol, no additional water was added during the synthesis and crystal growth process. This suggests that the presence of a rigid secondary coordination environment may facilitate the preorganization of water molecules.

Electrochemical characterization

The electrochemical properties were investigated by cyclic voltammetry (CV) and differential pulse voltammetry (DPV) to ensure that the existence of the pocket ligand will not affect the redox process of **1** compared with the reference molecule **2**, so as to ensure that we can reasonably use this model to stabilize the preorganized seven-coordinate aqua ligand to allow for its characterization. Three oxidation potentials around 0.71, 1.19, and 1.36 V versus normal hydrogen electrode (NHE) were observed (Supporting Information Figure S7), which were assigned to three consecutive one-electron-transfer processes Ru^{II}→Ru^{III}→Ru^{IV}→Ru^V. This electron transfer process was also confirmed by the Pourbaix diagram (Supporting Information Figure S8). Once the Ru^V oxidation state is reached, a dramatic current increase is observed, attributed to the water oxidation process. Similar electrochemical behavior was also recorded for reference **2**. To investigate what happens to the macrocyclic ligand at higher oxidation states, DFT calculations were performed. The optimized structures of **1** at Ru^{IV} and Ru^V states are depicted in Supporting Information Figure S9. The results indicate that the macrocyclic ligand rotates in the direction of carboxylates at higher oxidation states, which is conducive to the subsequent O–O formation.

Characterization of Ru^{III} aqua complex

As one aqua ligand was clearly located in **1·H₂O** but not near the Ru^{II} center, we proceeded with considerable effort to isolate and crystallize the Ru^{III} intermediate (**1**⁺) to see if and how water molecules interact with its catalytic center. Complex **1** (Ru^{II}) could be oxidized to **1**⁺ (Ru^{III}) in the presence of Ce^{IV}, which is confirmed by HRMS (Figure 4b and Supporting Information Figure S10; calcd for C₃₀H₂₆N₄O₁₀Ru⁺, 704.0701; found, 704.0710) and UV-vis redox titration (Figure 4a). With the gradual addition of Ce^{IV} to **1**, the metal-to-ligand charge transfer absorptions at 400 and 506 nm are bleached, and the absorbance at 290 nm increases simultaneously with an isosbestic point at 348 nm. It is worth noting that no absorption band around 690 nm is observed, which was previously assigned to green Ru-dimer or -trimer formation, even when the solution was left under air for 1 day (Supporting Information Figure S11).^{36,44–48} Oligomerization of the catalyst is considered to be one of the main routes of catalyst decomposition, which is circumvented by introduction of these macrocyclic ligands.

The addition of excess aqueous NH₄PF₆ to the solution of **1**⁺ resulted in slow formation of orange needle-like crystals, and the crystal refinement is presented in Figures 5a and 5b. The obtained crystal of **1**⁺·3H₂O·CH₃CN·PF₆[−] is composed of one [Ru^{III}bda]⁺ cation, one [PF₆][−] counterion, one CH₃CN molecule, and

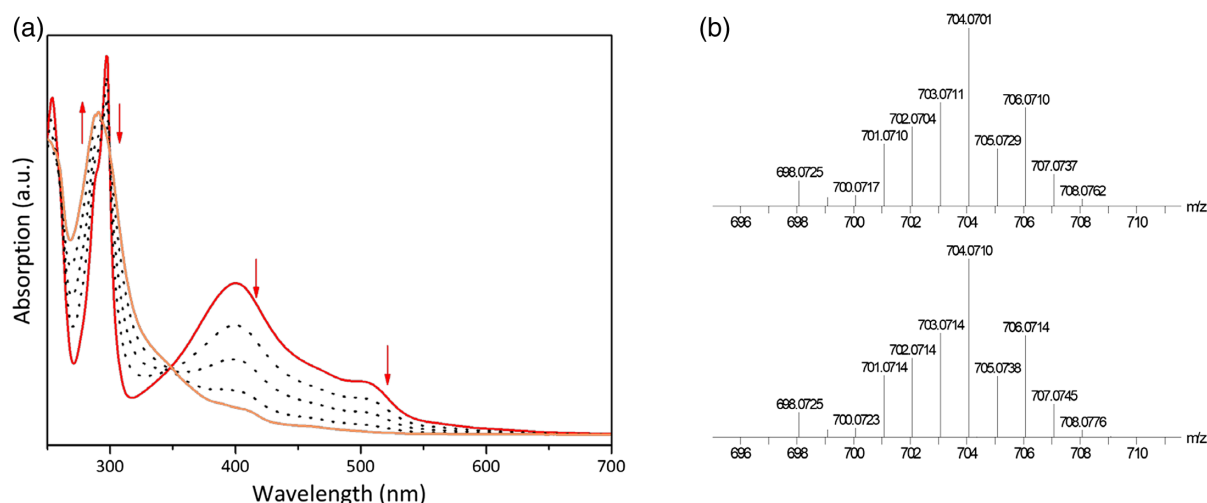


Figure 4 | (a) UV-vis spectra of **1** in the presence of increasing addition of Ce^{IV} (0–1 equiv) in 1:10 $\text{CF}_3\text{CH}_2\text{OH}$ /water (pH 1, trifluoromethane sulfonic acid); (b) HRMS of **1**⁺ (lower) and calculated mass spectrum (upper).

three adjacent water molecules in one unit cell. The structural differences between **1** and **1**⁺ are the increase of the O–Ru–O angle from 122.9° to 126.2°, as well as the inner $\text{N}_{\text{axial}}\text{–Ru–N}_{\text{axial}}$ angle from 169.0° to 170.5°. Those larger angles facilitate accommodation of the incoming seven-coordinate aqua ligand. To our delight, indeed a trapped water molecule (W_3) near the Ru center was captured with a $\text{Ru}\cdots\text{O}(\text{W}_3)$ distance of only 3.62 Å (the sum of van der Waals radii for Ru and O is about 3.60–4.08 Å),⁴⁹ which indicates there should be weak interaction between them. To the best of our knowledge, this is the shortest $\text{Ru}^{\text{III}}\cdots\text{aqua}$ distance found for any analogue of the Ru-bda family. In addition, the oxygen atom of W_3 nearly bisects the O–Ru–O angle, which convinces us that W_3 is effectively preorganized for coordination with the Ru center. Taken together the above data indicate that W_3 is likely a “ready-to-go” seven-coordinate ligand. In addition, the steric effect of the macrocyclic ligand was checked by topographic steric maps (Supporting Information Figure S12).^{50–52} Similar hindrances around catalytic sites were obtained from **1**⁺ and $\text{Ru}^{\text{III}}(\text{bda})\text{pic}_2$, suggesting that the existence of the pocket ligand provided no further steric hindrance to substrate binding and reactions.

Theoretical investigation

The proposed pseudo seven-coordinate Ru^{III} aqua complex, denoted as $\text{Ru}^{\text{III}}\cdots\text{OH}_2$, was furthermore examined by DFT calculations. Three water molecules were involved in optimizing the conformation of $\text{Ru}^{\text{III}}\cdots\text{OH}_2$ due to the same situation found in crystal structure. The calculated distance of $\text{Ru}\cdots\text{O}$ (3.53 Å, the closest water) is similar to that of the single crystal, as shown in Supporting Information Figure S13a. Since the catalysis

occurred in an aqueous microenvironment, one more water molecule was added to investigate the influence of solvent. A minor change in the solvent environment could alter the interaction between Ru and incoming aqua ligand as indicated by the decreased $\text{Ru}\cdots\text{O}$ distance of 3.35 Å (Supporting Information Figure S13b), which suggests that the seven-coordinated $\text{Ru}^{\text{III}}\text{–OH}_2$ was likely present in the catalytic cycle. In addition, two structures of Ru^{III} complex with three water molecules shown in Supporting Information Figures S18a and 18b were optimized in approaching and bonding modes as reported in our previous study.³⁷ The atoms in molecules (AIM) and NCI analyses on the bonding mode complex (Supporting Information Figures S18b1 and S18b2) indicate that the incoming water molecule has strong interaction and was bonded to the Ru center of the catalyst, which shows a bonding mode $\text{Ru}^{\text{III}}\text{–OH}_2$ complex. The other structure in the approaching mode, which originated from the crystal, has weak van der Waals interaction, but no bond between the incoming water and Ru center (Supporting Information Figures S18a1 and 18a2). In addition, the water molecules can establish H-bonds network inside the pocket, which might benefit further catalytic reactions.³² Graphical representations (Supporting Information Figure S18) and more detail about the interactions between the catalyst and water molecules are provided in Supporting Information.

Molecular dynamics (MD) calculations were conducted to further comprehend the influence of involving the macrocyclic ligand into the classic Ru-bda type catalyst. During the 100 ns MD calculations at the $\text{Ru}^{\text{V}}(\text{O})$ state, the macrocyclic ligand can rotate flexibly in front of the bda unit. The average H-bonds formed between the terminal O of $\text{Ru}^{\text{V}}(\text{O})$ and the water solvent is 0.014, and this hydrophobic nature is consistent with our previous

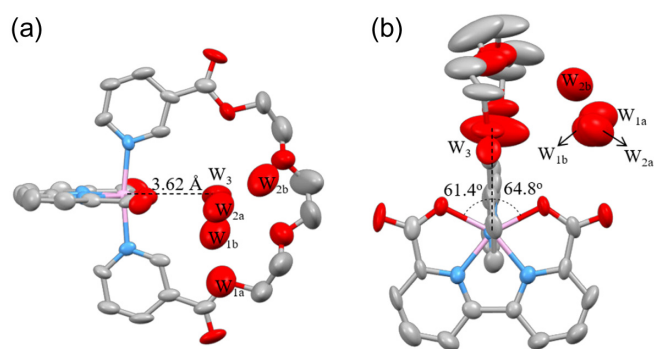


Figure 5 | Single-crystal structure of complex $1^+ \cdot 3\text{H}_2\text{O} \cdot \text{CH}_3\text{CN} \cdot \text{PF}_6^-$ [(a) side view and (b) top view] with thermal ellipsoids at 50% probability. Hydrogen, acetonitrile, and PF_6^- anion are omitted for clarity. Color code: Ru, pink; O, red; N, blue; C, grey.

studies.^{8–10} The radial distribution function of the terminal O (Supporting Information Figure S14) showed that the first solvation shells were at 3.2 and 3.0 Å for $\text{Ru}^{\text{V}}(\text{O})$ with and without macrocyclic ligand respectively, indicating that the addition of the macrocyclic ligands still maintained access to the water molecule to $\text{Ru}^{\text{V}}(\text{O})$ and imposed little effect on water approaching the $\text{Ru}^{\text{V}}(\text{O})$. Given the steric hindrance to coupling two $\text{Ru}^{\text{V}}(\text{O})$ units caused by macrocyclic ligands, the catalytic mechanism switched from interaction of two metal-oxo entities (I2M) to water nucleophilic attack (WNA) (Supporting Information Figure S15 and Table S2); however, that is beyond the scope of this work. Detailed catalytic water oxidation performance data can be found in Supporting Information.

Determining hydrogen-bonding network around catalytic site

Considering the split positions of $W_{1a/b}$ and $W_{2a/b}$ at $1^+ \cdot 3\text{H}_2\text{O} \cdot \text{CH}_3\text{CN} \cdot \text{PF}_6^-$ and the similar positions among W_1 of $1 \cdot \text{H}_2\text{O}$, W_{1b} and W_{2a} of $1^+ \cdot 3\text{H}_2\text{O} \cdot \text{CH}_3\text{CN} \cdot \text{PF}_6^-$, we

therefore suggest that $W_{1a/b}$ through $W_{2a/b}$ positions may act as the watergate through which aqua ligands coordinate to the catalyst active site during water oxidation. Therefore, to further investigate how the water molecules in the crystal interact with Ru-bda and each other, we conducted Hirshfeld surface analyses.⁵³ Hirshfeld surface analyses were employed to offer a global visualization of the intermolecular interactions in the crystal structures of $1 \cdot \text{H}_2\text{O}$ and $1^+ \cdot 3\text{H}_2\text{O} \cdot \text{CH}_3\text{CN} \cdot \text{PF}_6^-$. W_1 of $1 \cdot \text{H}_2\text{O}$ was fixed between a bda-carboxyl group and the macrocyclic ligand by hydrogen-bonding interactions (Supporting Information Figure S16, red spots), whereas $W_{1a/b}$ of $1^+ \cdot 3\text{H}_2\text{O} \cdot \text{CH}_3\text{CN} \cdot \text{PF}_6^-$ only strongly bonded to the neighboring $W_{2a/b}$ (Figure 6b). $W_{1a/b}$, $W_{2a/b}$, and W_3 of $1^+ \cdot 3\text{H}_2\text{O} \cdot \text{CH}_3\text{CN} \cdot \text{PF}_6^-$ strongly hydrogen bonded to each other, forming a hydrogen-bonding network (Figures 6b–6d). Interestingly, the “ready-to-go” aqua ligand W_3 also showed strong affinities to H_d and O of the macrocyclic ligand with hydrogen-bond distances in the range of 2.4–2.7 Å (Figure 6a and Supporting Information Figure S17), which means that the semifixed coordination environment contributes considerably to capturing this aqua ligand. Hydrogen-bonded water networks play important roles in lowering the transition state (TS) energy in artificial photosynthetic systems and facilitate proton/electron transfer in natural photosynthesis.^{39,54,55} The water channel observed here offers a structural model to understand the mechanism of water coordination/transfer pathways.

Conclusions

A new Ru-bda type water oxidation catalyst was tailor-made and carefully studied as a model system to detail the water coordination pathway, and four vital points from this work are worth highlighting:

- (1) For the first time, a “ready-to-go” pseudo seven-coordinate aqua ligand was captured at the Ru^{III} state, which means minimum structural change is

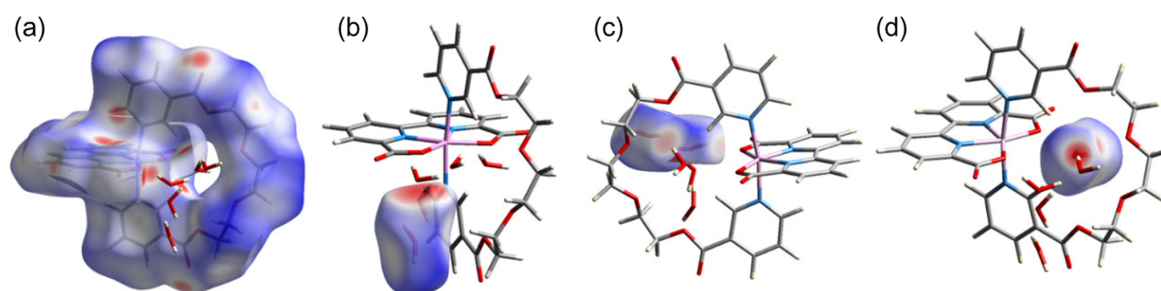


Figure 6 | Hirshfeld surface for (a) $\text{Ru}^{\text{III}}\text{bda}$ cation, (b) $W_{1a/b}$, (c) $W_{2a/b}$, and (d) W_3 in 1^+ mapped with normalized contact distance (d_{norm}) from red (distances shorter than sum of van der Waals radii) through white to blue (distances longer than sum of van der Waals radii). Color code: Ru, pink; O, red; N, blue; C, grey; H, white.

needed to shuttle substrate water molecules close to the catalytic center.

- (2) A formed hydrogen-bonding network near Ru was observed. Although hydrogen-bonding networks have been found earlier in the crystal structure of many molecular water oxidation catalysts, here an aqua ligand is located a viable distance from the catalytic site.
- (3) The introduction of macrocyclic ligands retain similar fundamental hydrophobicity and solvent exposure of $\text{Ru}^{\text{V}}(\text{O})$, from which we envisage its water oxidation catalytic performance.
- (4) Our approach constitutes a promising model system for studying processes near the catalytic site, which is also one of the motivations for this project. By replacing different types of linker between two axial ligands, this model can be further developed to study how the local hydrophobic/hydrophilic environment influences water oxidation activities and how the incorporation of redox-active/inactive metal ions affects the catalytic sites.

In summary, to close the catalytic cycle, a pocket-shaped pseudo seven-coordinate Ru^{III} -bda with a “ready-to-go” aqua ligand was isolated and clearly characterized by single-crystal X-ray diffraction. It is the first time visualizing how the Ru-based water oxidation catalyst captures substrate aqua ligands from bulk water through a hydrogen-bonding network. The strategies presented may also serve to inspire investigation of other types of Ru-based catalysis where the catalytic center attains coordination number seven at certain stages.

Supporting Information

Supporting Information is available and includes the general information, experimental methods, computational details, xyz coordinates of optimized structures, and copies of NMR and HRMS spectra.

Conflict of Interest

There is no conflict of interest to report.

Funding Information

We would like to thank Prof. Xiaoying Huang (Fujian Institute of Research on the Structure of Matter) and Dr. A. Ken Inge (Stockholm University) for assistance with single crystal refinements; Assoc. Prof. Zoltán Szabó (KTH) for NMR analyses; Dinghua Zhou (DUT) for HRMS measurements; Yi Yang (KTH) for ICP-OES measurements; Assoc. Prof. Lele Duan (SUSTech) and Prof. Fusheng Li (DUT) for comments on the manuscript. Special thanks go to Dr. Yinjuan Chen and Dr. Xiaohuo Shi

(Instrumentation and Service Center for Molecular Sciences at Westlake University) for supporting in HRMS and NMR measurements.

Acknowledgments

This work was financially supported by the Swedish Research Council (2017-00935), the Knut and Alice Wallenberg Foundation (KAW 2016.0072), and the China Scholarship Council (CSC). The authors would like to thank Prof. Xiaoying Huang (Fujian Institute of Research on the Structure of Matter) and Dr. A. Ken Inge (Stockholm University) for assistance with single-crystal refinements; Dinghua Zhou (DUT) and Dr. Yinjuan Chen (Westlake University) for HR-MS measurements; Yi Yang (KTH) for ICP-OES measurements; and Assoc. Prof. Lele Duan at SUSTech and Assoc. Prof. Fusheng Li at DUT for comments on the manuscript.

References

1. Kärkäs, M. D.; Verho, O.; Johnston, E. V.; Åkermark, B. R. Artificial Photosynthesis: Molecular Systems for Catalytic Water Oxidation. *Chem. Rev.* **2014**, *114*, 11863–12001.
2. Zhang, B.; Sun, L. Artificial Photosynthesis: Opportunities and Challenges of Molecular Catalysts. *Chem. Soc. Rev.* **2019**, *48*, 2216–2264.
3. Garrido-Barros, P.; Gimbert-Suriñach, C.; Matheu, R.; Sala, X.; Llobet, A. How to Make an Efficient and Robust Molecular Catalyst for Water Oxidation. *Chem. Soc. Rev.* **2017**, *46*, 6088–6098.
4. Gilbert, J. A.; Eggleston, D. S.; Murphy, W. R.; Geselowitz, D. A.; Gersten, S. W.; Hodgson, D. J.; Meyer, T. J. Structure and Redox Properties of the Water-Oxidation Catalyst $[(\text{bpy})_2(\text{OH}_2)\text{RuORu}(\text{OH}_2)(\text{bpy})_2]^{4+}$. *J. Am. Chem. Soc.* **1985**, *107*, 3855–3864.
5. Zong, R.; Thummel, R. P. A New Family of Ru Complexes for Water Oxidation. *J. Am. Chem. Soc.* **2005**, *127*, 12802–12803.
6. Duan, L.; Bozoglian, F.; Mandal, S.; Stewart, B.; Privalov, T.; Llobet, A.; Sun, L. A Molecular Ruthenium Catalyst with Water-Oxidation Activity Comparable to that of Photosystem II. *Nat. Chem.* **2012**, *4*, 418–423.
7. Zhan, S.; Zou, R.; Ahlquist, M. R. S. Dynamics with Explicit Solvation Reveals Formation of the Prereactive Dimer as Sole Determining Factor for the Efficiency of Ru (bda) L_2 Catalysts. *ACS Catal.* **2018**, *8*, 8642–8648.
8. Zhan, S.; Mårtensson, D.; Purg, M.; Kamerlin, S. C.; Ahlquist, M. S. Capturing the Role of Explicit Solvent in the Dimerization of $\text{Ru}^{\text{V}}(\text{bda})$ Water Oxidation Catalysts. *Angew. Chem. Int. Ed.* **2017**, *56*, 6962–6965.
9. Zhan, S.; Zhang, B.; Sun, L.; Ahlquist, M. S. Hydrophobic/Hydrophilic Directionality Affects the Mechanism of Ru-Catalyzed Water Oxidation Reaction. *ACS Catal.* **2020**, *10*, 13364–13370.

10. Zhan, S.; Ahlquist, M. S. Dynamics and Reactions of Molecular Ru Catalysts at Carbon Nanotube–Water Interfaces. *J. Am. Chem. Soc.* **2018**, *140*, 7498–7503.
11. Richmond, C. J.; Escayola, S.; Poater, A. Axial Ligand Effects of Ru-BDA Complexes in the O–O Bond Formation via the I2M Bimolecular Mechanism in Water Oxidation Catalysis. *Eur. J. Inorg. Chem.* **2019**, *2019*, 2101–2108.
12. Richmond, C. J.; Matheu, R.; Poater, A.; Falivene, L.; Benet-Buchholz, J.; Sala, X.; Cavallo, L.; Llobet, A. Supramolecular Water Oxidation with Ru-bda-Based Catalysts. *Chem. Eur. J.* **2014**, *20*, 17282–17286.
13. Xie, Y.; Shaffer, D. W.; Concepcion, J. J. O–O Radical Coupling: From Detailed Mechanistic Understanding to Enhanced Water Oxidation Catalysis. *Inorg. Chem.* **2018**, *57*, 10533–10542.
14. Fan, T.; Zhan, S.; Ahlquist, M. S. Why Is There a Barrier in the Coupling of Two Radicals in the Water Oxidation Reaction? *ACS Catal.* **2016**, *6*, 8308–8312.
15. Shaffer, D. W.; Xie, Y.; Szalda, D. J.; Concepcion, J. J. Manipulating the Rate-Limiting Step in Water Oxidation Catalysis by Ruthenium Bipyridine-Dicarboxylate Complexes. *Inorg. Chem.* **2016**, *55*, 12024–12035.
16. Matheu, R.; Garrido-Barros, P.; Gil-Sepulcre, M.; Ertem, M. Z.; Sala, X.; Gimbert-Suriñach, C.; Llobet, A. The Development of Molecular Water Oxidation Catalysts. *Nat. Rev. Chem.* **2019**, *3*, 331–341.
17. Zhang, B.; Sun, L. Ru-bda: Unique Molecular Water-Oxidation Catalysts with Distortion Induced Open Site and Negatively Charged Ligands. *J. Am. Chem. Soc.* **2019**, *141*, 5565–5580.
18. Duan, L.; Wang, L.; Li, F.; Li, F.; Sun, L. Highly Efficient Bioinspired Molecular Ru Water Oxidation Catalysts with Negatively Charged Backbone Ligands. *Acc. Chem. Res.* **2015**, *48*, 2084–2096.
19. Luque-Urrutia, J. A.; Kamdar, J. M.; Grotjahn, D. B.; Solà, M.; Poater, A. Understanding the Performance of a Bisphosphonate Ru Water Oxidation Catalyst. *Dalton Trans.* **2020**, *49*, 14052–14060.
20. Xie, Y.; Shaffer, D. W.; Lewandowska-Andralojc, A.; Szalda, D. J.; Concepcion, J. J. Water Oxidation by Ruthenium Complexes Incorporating Multifunctional Bipyridyl Diphosphonate Ligands. *Angew. Chem. Int. Ed.* **2016**, *55*, 8067–8071.
21. Kamdar, J. M.; Marelus, D. C.; Moore, C. E.; Rheingold, A. L.; Smith, D. K.; Grotjahn, D. B. Ruthenium Complexes of 2, 2'-Bipyridine-6,6'-diphosphonate Ligands for Water Oxidation. *ChemCatChem* **2016**, *8*, 3045–3049.
22. Shaffer, D. W.; Xie, Y.; Szalda, D. J.; Concepcion, J. J. Lability and Basicity of Bipyridine-Carboxylate-Phosphonate Ligand Accelerate Single-Site Water Oxidation by Ruthenium-Based Molecular Catalysts. *J. Am. Chem. Soc.* **2017**, *139*, 15347–15355.
23. Matheu, R.; Ertem, M. Z.; Benet-Buchholz, J.; Coronado, E.; Batista, V. S.; Sala, X.; Llobet, A. Intramolecular Proton Transfer Boosts Water Oxidation Catalyzed by a Ru Complex. *J. Am. Chem. Soc.* **2015**, *137*, 10786–10795.
24. Yang, J.; Wang, L.; Zhan, S.; Zou, H.; Chen, H.; Ahlquist, M. S. G.; Duan, L.; Sun, L. From Ru-bda to Ru-bds: A Step Forward to Highly Efficient Molecular Water Oxidation Electrocatalysts Under Acidic and Neutral Conditions. *Nat. Commun.* **2021**, *12*, 373.
25. Shatskiy, A.; Bardin, A. A.; Oschmann, M.; Matheu, R.; Benet-Buchholz, J.; Eriksson, L.; Kärkäs, M. D.; Johnston, E. V.; Gimbert-Suriñach, C.; Llobet, A.; Åkermark, B. Electrochemically Driven Water Oxidation by a Highly Active Ruthenium-Based Catalyst. *ChemSusChem* **2019**, *12*, 2251–2262.
26. Liu, Y.; Ng, S.-M.; Yiu, S.-M.; Lam, W. W. Y.; Wei, X.-G.; Lau, K.-C.; Lau, T.-C. Catalytic Water Oxidation by Ruthenium(II) Quaterpyridine (qpy) Complexes: Evidence for Ruthenium(III) qpy-N,N''-dioxide as the Real Catalysts. *Angew. Chem. Int. Ed.* **2014**, *53*, 14468–14471.
27. Zong, R.; Thummel, R. P. 2,9-Di-(2'-pyridyl)-1,10-phenanthroline: A Tetradentate Ligand for Ru(II). *J. Am. Chem. Soc.* **2004**, *126*, 10800–10801.
28. Muckerman, J. T.; Kowalczyk, M.; Badieli, Y. M.; Polyansky, D. E.; Concepcion, J. J.; Zong, R.; Thummel, R. P.; Fujita, E. New Water Oxidation Chemistry of a Seven-Coordinate Ruthenium Complex with a Tetradentate Polypyridyl Ligand. *Inorg. Chem.* **2014**, *53*, 6904–6913.
29. Tseng, H.-W.; Zong, R.; Muckerman, J. T.; Thummel, R. Mononuclear Ruthenium(II) Complexes that Catalyze Water Oxidation. *Inorg. Chem.* **2008**, *47*, 11763–11773.
30. Zhang, G.; Zong, R.; Tseng, H.-W.; Thummel, R. P. Ru(II) Complexes of Tetradentate Ligands Related to 2,9-Di(pyrid-2'-yl)-1,10-phenanthroline. *Inorg. Chem.* **2008**, *47*, 990–998.
31. Shaffer, D. W.; Xie, Y.; Concepcion, J. J. O–O Bond Formation in Ruthenium-Catalyzed Water Oxidation: Single-Site Nucleophilic Attack vs. O–O Radical Coupling. *Chem. Soc. Rev.* **2017**, *46*, 6170–6193.
32. Schulze, M.; Kunz, V.; Frischmann, P. D.; Würthner, F. A Supramolecular Ruthenium Macrocyclic with High Catalytic Activity for Water Oxidation that Mechanistically Mimics Photosystem II. *Nat. Chem.* **2016**, *8*, 576.
33. Wang, L.; Duan, L.; Wang, Y.; Ahlquist, M. S.; Sun, L. Highly Efficient and Robust Molecular Water Oxidation Catalysts Based on Ruthenium Complexes. *Chem. Commun.* **2014**, *50*, 12947–12950.
34. Duan, L.; Fischer, A.; Xu, Y.; Sun, L. Isolated Seven-Coordinate Ru(IV) Dimer Complex with [HOHOH][−] Bridging Ligand as an Intermediate for Catalytic Water Oxidation. *J. Am. Chem. Soc.* **2009**, *131*, 10397–10399.
35. Lebedev, D.; Pineda-Galvan, Y.; Tokimaru, Y.; Fedorov, A.; Kaeffer, N.; Copéret, C.; Pushkar, Y. The Key Ru^V=O Intermediate of Site-Isolated Mononuclear Water Oxidation Catalyst Detected by in Situ X-Ray Absorption Spectroscopy. *J. Am. Chem. Soc.* **2018**, *140*, 451–458.
36. Concepcion, J. J.; Zhong, D. K.; Szalda, D. J.; Muckerman, J. T.; Fujita, E. Mechanism of Water Oxidation by [Ru(bda)(L)₂]: The Return of the “Blue Dimer”. *Chem. Commun.* **2015**, *51*, 4105–4108.
37. Daniel, Q.; Huang, P.; Fan, T.; Wang, Y.; Duan, L.; Wang, L.; Li, F.; Rinkevicius, Z.; Mamedov, F.; Ahlquist, M. S. Rearranging from 6- to 7-Coordination Initiates the Catalytic

Activity: An EPR Study on a Ru-bda Water Oxidation Catalyst. *Coord. Chem. Rev.* **2017**, *346*, 206–215.

38. Matheu, R.; Ghaderian, A.; Francàs, L.; Chernev, P.; Ertem, M. Z.; Benet-Buchholz, J.; Batista, V. S.; Haumann, M.; Gimbert-Suriñach, C.; Sala, X. Behavior of Ru-bda Water-Oxidation Catalysts in Low Oxidation States. *Chem. Eur. J.* **2018**, *24*, 12838–12847.

39. Kern, J.; Chatterjee, R.; Young, I. D.; Fuller, F. D.; Lassalle, L.; Ibrahim, M.; Gul, S.; Fransson, T.; Brewster, A. S.; Alonso-Mori, R. Structures of the Intermediates of Kok's Photosynthetic Water Oxidation Clock. *Nature* **2018**, *563*, 421–425.

40. Zhao, L.; Jing, X.; Li, X.; Guo, X.; Zeng, L.; He, C.; Duan, C. Catalytic Properties of Chemical Transformation within the Confined Pockets of Werner-Type Capsules. *Coord. Chem. Rev.* **2019**, *378*, 151–187.

41. Kunz, V.; Lindner, J. O.; Schulze, M.; Röhr, M. I.; Schmidt, D.; Mitrić, R.; Würthner, F. Cooperative Water Oxidation Catalysis in a Series of Trinuclear Metallosupramolecular Ruthenium Macrocycles. *Energy. Environ. Sci.* **2017**, *10*, 2137–2153.

42. Meza-Chincha, A.-L.; Lindner, J. O.; Schindler, D.; Schmidt, D.; Krause, A.-M.; Röhr, M. I. S.; Mitrić, R.; Würthner, F. Impact of Substituents on Molecular Properties and Catalytic Activities of Trinuclear Ru Macrocycles in Water Oxidation. *Chem. Sci.* **2020**, *11*, 7654–7664.

43. Gao, Y.; Ding, X.; Liu, J.; Wang, L.; Lu, Z.; Li, L.; Sun, L. Visible Light Driven Water Splitting in a Molecular Device with Unprecedentedly High Photocurrent Density. *J. Am. Chem. Soc.* **2013**, *135*, 4219–4222.

44. Zhang, B.; Li, F.; Zhang, R.; Ma, C.; Chen, L.; Sun, L. Characterization of a Trinuclear Ruthenium Species in Catalytic Water Oxidation by Ru(bda)(pic)₂ in Neutral Media. *Chem. Commun.* **2016**, *52*, 8619–8622.

45. Yang, Q.-Q.; Jiang, X.; Yang, B.; Wang, Y.; Tung, C.-H.; Wu, L.-Z. Amphiphilic Oxo-Bridged Ruthenium “Green Dimer” for Water Oxidation. *iScience* **2020**, *23*, 100969.

46. Wang, D.; Sampaio, R. N.; Troian-Gautier, L.; Marquard, S. L.; Farnum, B. H.; Sherman, B. D.; Sheridan, M. V.; Dares, C. J.; Meyer, G. J.; Meyer, T. J. Molecular Photoelectrode for Water Oxidation Inspired by Photosystem II. *J. Am. Chem. Soc.* **2019**, *141*, 7926–7933.

47. Yang, J.; An, J.; Tong, L.; Long, B.; Fan, T.; Duan, L. Sulfur Coordination Effects on the Stability and Activity of a Ruthenium-Based Water Oxidation Catalyst. *Inorg. Chem.* **2019**, *58*, 3137–3144.

48. Luque-Urrutia, J. A.; Solà, M.; Poater, A. The Influence of the pH on the Reaction Mechanism of Water Oxidation by a Ru(bda) Catalyst. *Catal. Today* **2020**, *358*, 278–283.

49. Batsanov, S. Van der Waals Radii of Elements. *Inorg. Mater.* **2001**, *37*, 871–885.

50. Falivene, L.; Cao, Z.; Petta, A.; Serra, L.; Poater, A.; Oliva, R.; Scarano, V.; Cavallo, L. Towards the Online Computer-Aided Design of Catalytic Pockets. *Nat. Chem.* **2019**, *11*, 872–879.

51. Poater, A.; Ragone, F.; Giudice, S.; Costabile, C.; Dorta, R.; Nolan, S. P.; Cavallo, L. Thermodynamics of N-Heterocyclic Carbene Dimerization: The Balance of Sterics and Electronics. *Organometallics* **2008**, *27*, 2679–2681.

52. Poater, A.; Ragone, F.; Mariz, R.; Dorta, R.; Cavallo, L. Comparing the Enantioselective Power of Steric and Electrostatic Effects in Transition-Metal-Catalyzed Asymmetric Synthesis. *Chem. Eur. J.* **2010**, *16*, 14348–14353.

53. Spackman, M. A.; Jayatilaka, D. Hirshfeld Surface Analysis. *CrystEngComm* **2009**, *11*, 19–32.

54. Vigara, L.; Ertem, M. Z.; Planas, N.; Bozoglian, F.; Leidel, N.; Dau, H.; Haumann, M.; Gagliardi, L.; Cramer, C. J.; Llobet, A. Experimental and Quantum Chemical Characterization of the Water Oxidation Cycle Catalyzed by [RuII(damp)(bpy)(H₂O)]²⁺. *Chem. Sci.* **2012**, *3*, 2576–2586.

55. Umena, Y.; Kawakami, K.; Shen, J.-R.; Kamiya, N. Crystal Structure of Oxygen-Evolving Photosystem II at a Resolution of 1.9 Å. *Nature* **2011**, *473*, 55–60.